ISSN 1075-7015, Geology of Ore Deposits, 2019, Vol. 61, No. 7, pp. 637–646. © Pleiades Publishing, Ltd., 2019.
Russian Text © The Author(s), 2018, published in Zapiski Rossiiskogo Mineralogicheskogo Obshchestva, 2018, No. 3, pp. 44–59.

MINERALS AND MINERAL PARAGENESES

New Data on Chemical Composition and Vibrational Spectra of Magnetoplumbite-Group Minerals

N. V. Chukanov[a, b, *], S. S. Vorobei[a], V. N. Ermolaeva[c, d], D. A. Varlamov[b, c], P. Y. Plechov[a, e], S. Jančev[f], and A. V. Bovkun[a]

[a] *Geological Faculty, Moscow State University, Moscow, 119991 Russia*
[b] *Institute of Problems of Chemical Physics, Russian Academy of Sciences, Chernogolovka, Moscow Oblast, 142432 Russia*
[c] *Institute of Experimental Mineralogy, Russian Academy of Sciences, Chernogolovka, Moscow Oblast, 142432 Russia*
[d] *Institute of Geochemistry and Analytical Chemistry, Russian Academy of Sciences, Moscow, 119991 Russia*
[e] *Fersman Mineralogical Museum, Russian Academy of Sciences, Moscow, 119071 Russia*
[f] *Faculty of Technology and Metallurgy, Saint Cyril and Methodius University, Skopje, 1000 Republic of North Macedonia*
**e-mail: chukanov@icp.ac.ru*

Received January 22, 2018; revised February 14, 2018; accepted February 14, 2018

Abstract—Magnetoplumbite-group minerals from various paragenetic assemblages, including a xenolith of altered garnet lherzolite from the Obnazhennaya kimberlite pipe in Yakutia, sulfide-free metasomatic Pb–Zn–Sb ore from the Pelagonian massif in the Republic of North Macedonia, and some other metasomatic occurrences have been studied with electron microprobe, as well as using IR and Raman spectroscopy. New data on isomorphic substitutions and crystal chemistry of the magnetoplumbite-group minerals have been obtained. Three potentially new mineral species belonging to this group have been identified: Al-dominant analogue of yimengite, Ba-dominant analogue of nežilovite, and Mn-dominant analogue of plumboferrite.

Keywords: magnetoplumbite group, isomorphism, metasomatites, Pelagonian massif, Obnazhennaya kimberlite pipe, IR spectroscopy, Raman spectroscopy

DOI: 10.1134/S1075701519070055

INTRODUCTION

An interest in the magnetoplumbite-group minerals (MGM) is related to both the presence of accessory constituents in various altered rocks and synthetic analogues of some of these minerals, which are widely used as ferrimagnets with high coercive field strength (Stäblen, 1982).

The magnetoplumbite group comprises isostructural hexagonal ($P6_3/mmc$) oxides with the general formula $AM_{12}O_9$, where A denotes large cations (Pb^{2+}. Ba, K, *REE*) or Fe^{2+}; M are small-radius cations with the coordination number from 4 to 6 (Fe^{3+}, Fe^{2+}, Mn^{4+}, Mn^{3+}, Mn^{2+}, Ti^{4+}, Cr^{3+}, Zn, Mg) and structurally related diaoyudaoite $NaAl_{11}O_{17}$, lindqvistite $Pb_2(Mn^{2+},Mg)$, and plumboferrite $Pb_2(Fe^{3+},Mn^{2+},Mg)_{11}O_{19-x}$ (Back, 2014) (Table 1). The MGM structures consist of two alternating blocks, R and S with the compositions $(AM_6O_{11})^{2-}$ and $(M_6O_8)^{2+}$, respectively (Townes et al., 1967; Obradors et al., 1985; Peng Zhizhong, Lu Qi, 1985; Haggerty et al., 1989; Bermanec et al., 1996; Grey et al., 1998; Lengauer et al., 2001). In the MGM with stoichiometry of proper magnetoplumbite, the M cations occupy five sites: octahedral $M(1)$, $M(4)$, and $M(5)$, tetrahedral $M(3)$, and $M(2)$ site which centers trigonal dipyramid. The A cation is surrounded by 12 oxygen atoms. The R block contains $M(2)$, $M(4)$, and $M(5)$ polyhedra with the $M(5)$ polyhedra sharing oxygen atoms with the neighboring R block. The neighboring $M(4)$ octahedra are face shared (the face is in the mirror plane at $z = 1/4$) to form a group (M_2O_9) that causes distortion of the $M(4)$ octahedron. As a result, in the structures of Ti-bearing MGM, Ti^{4+} predominantly concentrates at the $M(4)$ site. In the structures of magnetoplumbite and nežilovite, this site is also occupied by other high-valence cations with relatively small radii, Sb^{5+} and Mn^{4+}.

Plumboferrite and lindqvistite are structurally disordered and have vacancies at the oxygen sites as a result of incorporation of additional large cations (in plumboferrite up to 2 apfu Pb, $Z = 2$) into their structures. The idealized formula of plumboferrite may be written as $Pb(PbFe_{11})O_{19-x}$ (Holtstam et al., 1995).

Hibonite-(Fe) was described as a new mineral (Ma, 2010) without data on its crystal structure and iron valence. It is assumed that hibonite-(Fe) is a secondary mineral with Fe^{2+} instead of Ca. However, this

Table 1. MGM (Back, 2014)

Mineral	Formula ($Z = 2$)	Mineral	Formula ($Z = 2$)
Barioferrite	$BaFe^{3+}_{12}O_{12}$	Hibonite-(Fe)	$(Fe^{2+}, Mg)Al_{12}O_{19}$
Batiferrite	$BaTi_2Fe^{3+}_8Fe^{2+}_2O_{19}$	Lindqvistite	$Pb_2(Mn^{2+}, Mg)Fe^{3+}_{16}O_{27}$
Diaoyudaoite	$NaAl_{11}O_{17}$	Magnetoplumbite	$Pb(Fe^{3+}, Mn^{3+})_{12}O_{19}$
Haggertyite	$BaFe^{2+}_4Fe^{3+}_2Ti_5MgO_{19}$	Nežilovite	$PbZn_2Mn^{4+}_2Fe^{3+}_8O_{19}$
Hawthorneite	$BaMgTi_3Cr_4Fe^{2+}_2Fe^{3+}_2P_{19}$	Plumboferrite	$Pb_2(Fe^{3+}, Mn^{2+}, Mg)_{11}O_{19-x}$
Hibonite	$(Ca,Ce)(Al,Ti,Mg)_{12}O_{19}$	Yimengite	$K(Cr,Ti,Fe,Mg)_{12}O_{19}$

assumption is not consistent with the unit-cell parameters, which are greater than those of hibonite despite the ionic radius of Fe^{2+} being smaller than that of Ca^{2+}. It is assumed that hibonite-(Fe) could be formed as a result of Ca leaching from hibonite with sulfuric acid forming during oxidation of associated sulfide minerals. In this case, the *A* site can be occupied by H_2O or H_3O as indicated by the lowered total of electron-microprobe analysis (98.25 wt %) as compared to associated hibonite and weak band at 1600 cm^{-1} in the Raman spectrum. Nevertheless, additional studies are necessary to establish real origin of hibonite-(Fe).

The following topics were all studied here: compositional variations and vibration spectra of MGM including those of possible new mineral species from two mineral assemblages, deep xenoliths of altered garnet lherzolite from the Obnazhennaya pipe (yimengite and its Al-dominated analogue) and sulfide-free ore-bearing altered rocks of the Pelagonian massif in the Republic of North Macedonia (nežilovite, its Ba-dominate analogue, and Mn-domintated analogue of plumboferrite).

SAMPLE DESCRIPTION

Diverse MGM are typical accessory minerals of the ore-bearing metasomatic rocks at the contact of the Early Paleozoic metarhyolite and rhyolitic schist with dolomite marble and baryte schist in the vicinity of the Nežilovo village (Pelagonian massif, Republic of North Macedonia, see Barić (1960)). These metasomatic rocks are characterized by high contents of chalcophile elements (S, As, Sb, Zn, Pb, Cu). In contrast to the majority of endogenic polymetallic ores, these rocks are sulfide-free and contain chalcophile elements which are incorporated into oxygen-bearing compounds, predominantly oxides, silicates, phosphates, and arsenates. The mineral paragenetic assemblages of the ore-bearing metasomatic rocks were studied in detail (Chukanov et al., 2015, 2016, 2018; Ermolaeva et al., 2016, 2018; Jančev et al., 2016; Varlamov et al., 2017). It is concluded that the absence of sulfide minerals is caused by the high activity of Ba fixing sulfur in sulfate form and oxidative environment of the ore formation.

As a rule, accessory nežilovite is present in the fine- to medium-grained rocks composed predominantly by silicates (sample 2017-4), baryte with minor silicates (sample 2017-13), tilasite with silicates and carbonate veinlets (sample 9999B), ore calcite and dolomite with minor zinc spinels and silicates (sample bb). The Zn-bearing trioctahedral micas, amphiboles, pyroxenes, chlorites, talc, epidote supergroup minerals with variable contents of chalcophile elements (Pb, Zn, Cu), *REE*, Mn, and Fe, as well as feldspar and quartz, are the major silicate constituents of these rocks. The accessory mineralization is extremely diverse and includes gahnite, franklinite, zincochromite, braunite, zircon, ferricoronadite, various oxides of the högbomite and pyrochlore (including Sb-bearing) supergroups and magnetoplumbite and crichtonite groups. Baryte, minerals of the fluorapatite–hedyphane–mimetite series, calcite and dolomite are the typical constituents through all types of the Nežilovo sulfide-free ores.

Nežilovite occurs as black lamellar crystals with semimetal luster up to 2 mm across (Fig. 1). This mineral frequently forms fine epitaxial intergrowths with the högbomite-supergroup minerals, zincohögbomite, zincovelesite, and their Sb-analogues (Fig. 2).

The barium-dominated analogue of nežilovite occurs as zones within the crystals of nežilovite (Fig. 3). Judging from mosaic characters, it is assumed that zoning is caused by twining.

The manganese-dominated analogue of plumboferrite is present in the oxide assemblage of major minerals such as gahnite, franklinite, and zincovelesite-6*N*6*S* (sample FeCor-1). This sample is a fragment of the holotype zincovelesite-6*N*6*S* and ferricoronadite specimen (Chukanov et al., 2016, 2017). Here, Mn analogue of plumboferrite occurs as inclusion in the aggregate of the zincovelesite-6*N*6*S* lamellar crystals (Fig. 4).

The sample with the studied yimengite and its Al-dominant (Al > Cr) analogue came from the Obnazhennaya kimberlite pipe in the Kuoyoki down-

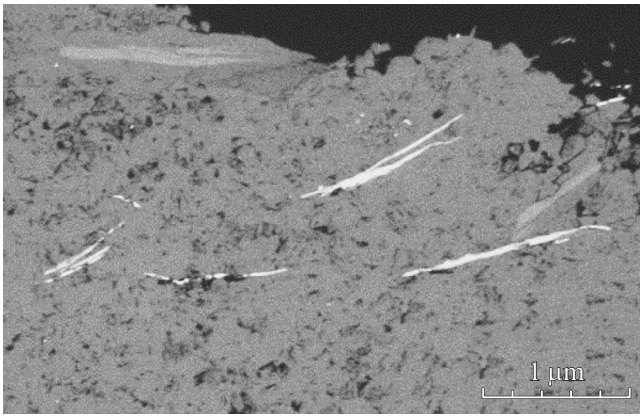

Fig. 1. Back-scattered electron image of nežilovite lamellae (white) in fine-grained dolomite-dominated rock with accessory phlogopite, talc, and braunite. Sample bb.

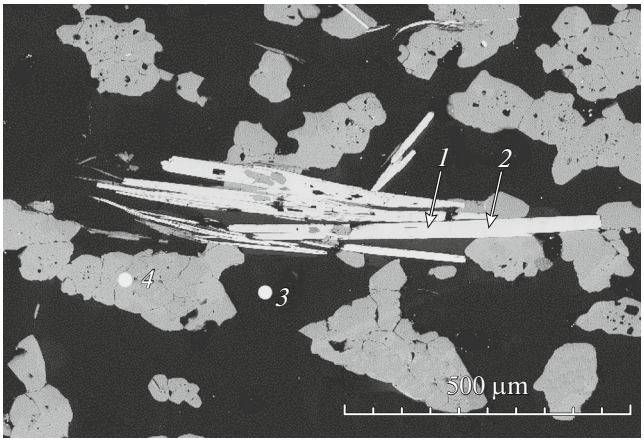

Fig. 3. Back-scattered electron image of nežilovite (light zones, (*1*) and nežilovite Ba analogue (dark zones, (*2*) in rock mainly composed of dolomite (*3*), with minor zinc spinels (*4*) and silicates. Sample bb. Polished section.

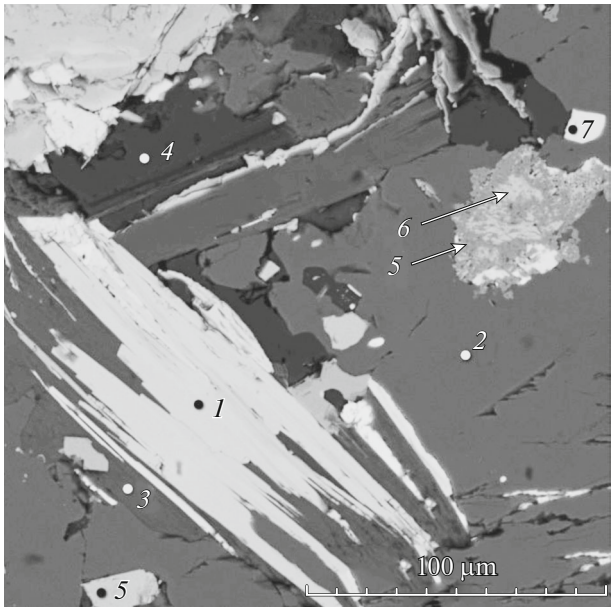

Fig. 2. Back-scattered electron image of fine nežilovite-zincovelesite epitaxial integrowth (*1*) in aegirine-augite, in association (*2*) with Zn-bearing phlogopite (*3*), albite (*4*), gahnite (*5*), franklinite (*6*), and baryte (*7*). Sample 2017-4. Polished section.

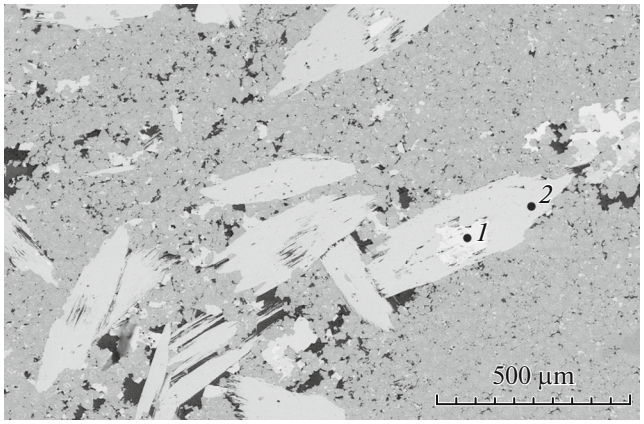

Fig. 4. Back-scattered electron image of inclusion of the Mn-analogue of plumboferrite (*1*) in zincovelesite (*2*), in association with gahnite, franklinite, ferricoronadite, and baryte. Sample FeCor-1. Polished section.

stream, Sakha-Yakutia, Russia and is a xenolith of garnet lherzolite of 2.6 × 1.4 cm in size. Garnet (30–35%), orthopyroxene (15–35%), clinopyroxene (10–30%), and olivine (10–20%) are the major constituents of this rock; Cr-rich spinel (up to 5%) is the major accessory constituent. The rock is massive with a hypidiomorhic texture.

Garnet occurs as magenta rounded isometric individuals up to 10 mm across; it is fractured and contains randomly oriented acicular inclusions of rutile up to 0.5 mm long. The garnet composition is predominantly pyrope; the relationship of pyrope, almandine, grossular, and knorringite endmembers is 66 : 16 : 12 : 6 (the Cr_2O_3 content is 2.3 wt %). The garnet grains have kelyphite rims 0.01 to 1 mm thick, which are composed of phlogopite tables. The irregular-shaped grains of *olivine* (Fo_{93}) range from 2 to 3.5 mm in size and are deeply serpentinized. The prismatic *orthopyroxene* crystals (enstatite containing approximately 4 wt % FeO and 2 wt % Al_2O_3) up to 10 mm long are partly replaced (in the rim and along fractures) by serpentine and carbonates. *Clinopyroxene* individuals are embedded into the crystals of orthopyroxene and are oriented along their cleavage (exsolution texture). Also rounded or prismatic clinopyroxene individuals ranging from 4 to 6 mm in size with embedded orthopyroxene (exsolution texture) and replaced by serpentine in the rim are observed. Clinopyroxene contains Al and Cr (approximately 15 and 5% of jadeite and kosmo-

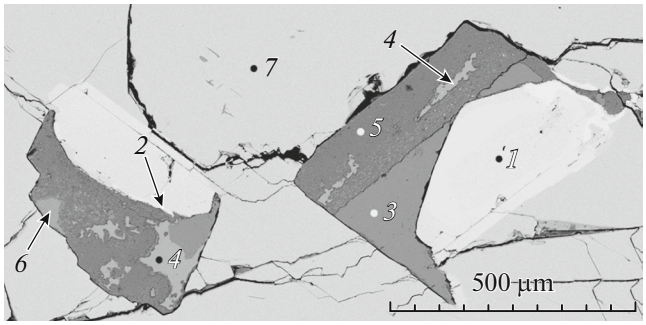

Fig. 5. Back-scattered electron image of polymineralic inclusions containing Al analogue of yimengite (*1*), mathiasite (*2*), dolomite (*3*), calcite (*4*), serpentine (*5*), and phlogopite (*6*) in Cr-rich spinel (*7*). Polished section.

chlor endmembers, respectively). The Cr-rich *spinel* occurs as irregular-shaped isotropic grains ranging from 0.5 to 10 mm in size. Ranges of the concentrations of different components are expressed by the formula $(Mg_{0.70}Fe_{0.29–0.30}Mn_{0–0.01})(Al_{0.97–1.12}Cr_{0.82–0.97}Fe_{0.05}Ti_{0.01})O_4$. Inclusions of carbonates, serpentine, phlogopite, mathiasite, yimengite, and Al-dominated yimengite analogue occur in the spinel grains (Figs. 5, 6). Maximal sizes of the mathiasite and K-dominated MGM individuals are 0.01 × 0.15 × 0.15 and 0.3 × 0.5 × 0.5 mm, respectively. The formation of these minerals is probably caused by rock alteration in mantle environment.

In addition, the following samples were used in this study for comparative spectroscopic study:

—hibonite, $Ca_{1.0}(Al_{10.2}Fe_{0.9}Ti_{0.6}Mg_{0.3})O_{19}$ from calc skarn of the Tashelga prospect in Gornaya Shoria, which forms brown tabular crystals of up to 0.2 × 1 × 1 cm in size associated with tashelgite, grossular, vesuvianite, magnetite, hercynite, corundum, apatite, perovskite, and diopside (Anan'ev et al., 2011);

—technogenic analogue of diaoyudaoite from slag of the Klyuchevskiy ferroalloy plant in Sverdlovsk Oblast, which is similar in the composition to the endmember of this mineral species;

—holotype sample of barioferrite (the empirical formula $Ba_{0.95}Fe^{+3}_{12.03}O_{19}$) from the Hartrurim Formation in Israel (inclusions in metamorphosed baryte concretion: Murashko et al. (2011));

—lindqvistite, $Pb_{2.0}(Fe_{14.8}Mn_{1.4}Mg_{0.8})O_{27}$ from skarn of the Jakobsberg deposit in Sweden (black tabular grains of up to 0.2 × 1 × 1 mm in size in association with jacobsite, phlogopite, andradite, and baryte);

—magnetoplumbite, $(Pb_{0.95}Ba_{0.05})(Fe_{8.1}Mn_{3.0}Ti_{0.8}Al_{0.1})O_{19}$ from skarn of the Långban deposit in Sweden (black irregular-shaped grains of up to 0.5 mm across associated with jacobsite, hematite, andradite, phlogopite, hedyphane, and calcite).

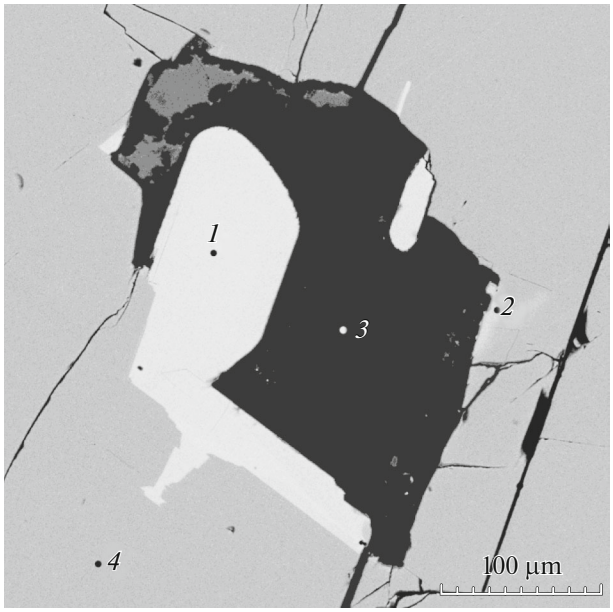

Fig. 6. Back-scattered electron image of polymineralic inclusion containing yimengite with zones of yimengite Al-analogue (*1*), rutile (*2*), and dolomite (*3*) in Cr-rich spinel (*4*). Polished section.

ANALYTICAL TECHNIQUES

The chemical composition has been determined on a Tescan Vega-II XMU scanning electron microscope equipped with EDS operated at acceleration voltage of 20 kV and current intensity 400 nA using an INCA Energy 450 system for registration of the X-ray radiation and calculation of the sample composition. The beam diameter was 157–180 nm (for the determination of the chemical composition) and 60 nm (for the back-scattered electron imaging). The more detailed description of this techniques is given in (Ermolaeva et al., 2016; Varlamov et al., 2017).

The Raman spectra were measured with an XPloRA (Horiba Scientific) Raman spectrometer equipped with a multichannel detector coupled with a confocal microscope including connective optics and optical filters. The focal distance of the spectrometer is 200 mm. Laser radiation with wavelength of 523 nm and rated power 25 mW was used. The measurements were done at close diaphragm decreasing power down to 10% of rated power to reduce effect of the laser beam on the sample. The measurements were done within the range of 100 to 2000 cm^{-1} using spectral lattice 2400T (2400 lines per mm). The acquisition time of each spectrum window was 90 s (three times by 30 s) in the mode of automatic merge of windows with the 100 line overlapping. The spectra were processed using the LabSpec program, version 5.78.24.

The infrared spectra of the MGM powders in the KBr pellets were measured on an ALPHA FTIR spectrometer Bruker Optics, Germany within the wave-

Table 2. Typical chemical compositions (wt %) of MGM and almeidaite from ore-bearing altered rocks of Nezilovo

Component	Mn-analogue of plumboferrite	Nežilovite		Ba-analogue of nežilovite	Almeidaite
BaO	B.d.l.	B.d.l.	B.d.l.	8.31	B.d.l.
PbO	32.29	17.71	17.89	7.70	11.76
CuO	B.d.l.	B.d.l.	0.94	B.d.l.	B.d.l.
ZnO	13.11	14.76	15.46	11.97	10.00
Fe_2O_3	16.84	40.55	43.15	43.33	15.95
Al_2O_3	B.d.l.	5.06	1.55	5.25	0.47
Ce_2O_3	″	B.d.l.	B.d.l.	B.d.l.	1.41
Mn_2O_3	23.20	″	″	″	8.11
MnO_2	B.d.l.	15.88	14.38	16.57	B.d.l.
TiO_2	16.30	4.10	8.59	6.27	51.37
ZrO_2	B.d.l.	B.d.l.	B.d.l.	B.d.l.	1.39
Sb_2O_5	0.42	2.13	″	″	0.83
Nb_2O_5	0.67	B.d.l.	″	″	B.d.l.
Total	103.55*	100.17	101.96	99.40	101.60
		Formula coefficients			
Ba	0	0	0	0.61	0
Pb	1.78	0.92	0.92	0.39	0.99
Ci	0	0	0.14	0	0
Zn	1.98	2.10	2.18	1.66	2.32
Fe	2.61	5.88	6.20	6.13	3.77
Al	0	1.15	0.35	1.16	0.17
Ce	0	0	0	0	0.16
Mn	3.64	2.12	1.90	2.15	2.16
Ti	2.51	0.59	1.23	0.89	12.13
Zr	0	0	0	0	0.21
Sb	0.03	0.15	0	0	0.09
Nb	0.06	0	0	0	0
Calculation basis	11 *M*-cations	12 *M*-cations	12 *M*-cations	12 *M*-cations	21 *M*-cations

B.d.l. denotes that the element content is below detection limit by electron microprobe; *high total may be caused by partial manganese in bivalence state and microrelief features of the analyzed grain.

number range of 360 to 3800 cm^{-1} with resolution of 4 cm^{-1} and scanning number of 16. Pure KBr pellet was used as reference material.

RESULTS

Chemical composition. The chemical compositions of MGM from Nezilovo and xenolith from the Obnazhennya pipe are given in Tables 2 and 3, respectively. The compositions of the crichtonite-group minerals (almeidaite and mathiasite) from the same mineral assemblages are given there too.

Nežilovite is the most abundant MGM in ore-bearing altered rocks of Nežilovo. It is present in various rock types but is characterized by a rather stable chemical composition.

The MGM from the Obnazhennaya pipe are fairly homogeneous in the chemical composition. The Cr : Al ratio is close to 1 : 1 in all analyzed points.

The characteristic compositional feature of the crichtonite-group minerals distinguishing them from MGM is a high Ti content. In addition, there are no vacancies at the *A* site of these minerals in contrast to yimengite and its Al analogue, which are characterized by the cation deficiency.

Raman spectroscopy. The Raman spectra of various MGM, yimengite Al-analogue, plumboferrite Mn-analogue, as well as hibonite and nežilovite (given for comparison), are shown in Fig. 7. In all spectra in

Table 3. Typical chemical compositions, wt % of MGM and mathiasite from Obnazhennaya kimberlite pipe

Component	Yimengite		Al-analogue of yimengite		Mathiasite
Na_2O	0.16	B.d.l.	B.d.l.	0.07	B.d.l.
K_2O	3.87	3.44	3.72	3.54	2.00
CaO	0.22	0.13	0.32	0.17	0.81
SrO	0.01	0.55	0.58	0.29	0.42
BaO	0.10	0.22	0.30	0.56	0.69
MgO	9.19	9.46	9.40	9.19	4.76
MnO	0.13	0.37	0.07	0.25	0.24
FeO	12.59	12.90	12.46	12.73	7.38
Al_2O_3	19.23	19.82	21.41	20.92	2.61
Cr_2O_3	31.57	30.11	29.91	29.18	12.38
TiO_2	22.83	23.62	21.42	22.86	70.15
Total	99.90	100.62	99.59	99.76	101.44
Formula coefficients					
Na	0.05	0	0	0.02	0
K	0.67	0.58	0.64	0.60	0.68
Ca	0.03	0.02	0.05	0.02	0.24
Sr	–	0.04	0.05	0.02	0.06
Ba	0.01	0.02	0.02	0.03	0.08
Mg	1.85	1.88	1.88	1.84	1.88
Mn	0.02	0.04	0.01	0.03	0.05
Fe	1.42	1.44	1.40	1.42	1.64
Al	3.05	3.11	3.38	3.31	0.82
Cr	3.36	3.17	3.17	3.09	2.60
Ti	2.31	2.36	2.16	2.31	14.01
Calculation basis	12 *M*-cations	12 *M*-cations	12 *M*-cations	12 *M*-cations	21 *M*-cations

the region above 900 cm^{-1}, only weak bands attributed to overtones and combination modes are observed. As expected, the increasing content of the lightest cations (Al and minor Mg) results in the shift of stretching vibrations involving cations at tetrahedral and bipyramidal coordination (range 500–900 cm^{-1}) to the high frequency region. This fact indicates the predominant incorporation of Al into the tetrahedrally coordinated *M* site.

The bands in the range of 200 to 500 cm^{-1} predominantly correspond to the vibrations involving octahedrally coordinated cations. The band at 122 cm^{-1} in the Raman spectrum of hibonite is assigned to Ca–O stretching vibrations. The bands of the similar K–O and Pb–O stretching vibrations of the other MGM whose spectra are shown in Fig. 7 are beyond the measured range in the lower frequency region because the force constants of the K–O and Pb–O bonds are much lower than that of Ca–O.

The highest frequency band in the Raman spectra of hibonite (at 879 cm^{-1}) is absent in the spectra of Al analogue of yimengite (with Al : Cr ≈ 1 : 1) and Mn-analogue of plumboferrite (Al-free MGM). However, in the Raman spectrum of nežilovite, a weak band with close wavenumber (at 865 cm^{-1}) is observed; it indicates possible clusters enriched in Al in tetrahedral and bipyramidal sites in this mineral.

The Al content in the Mn analogue of plumboferrite is below detection limit by electron microprobe. Thus, the rather weak high-frequency band at 769 cm^{-1} in the Raman spectrum of this mineral is caused by tetrahedrally coordinated cation with high force-strength characteristics in the mineral structure. Based on the chemical data for the Mn-analogue of plumboferrite (Table 2), one can assume that such cation is most likely Ti^{4+}. The incorporation of substantial Ti in this mineral and nežilovite is required by the charge balance constraints (charge compensation of Zn^{2+} ions, which partly replace Mn^{3+} and Fe^{3+}). This assumption is supported by the presence of a similar band (at 779 cm^{-1}) in the Raman spectrum of yimengite Al-analogue, which is most likely caused (judging from its high intensity) by the resonance

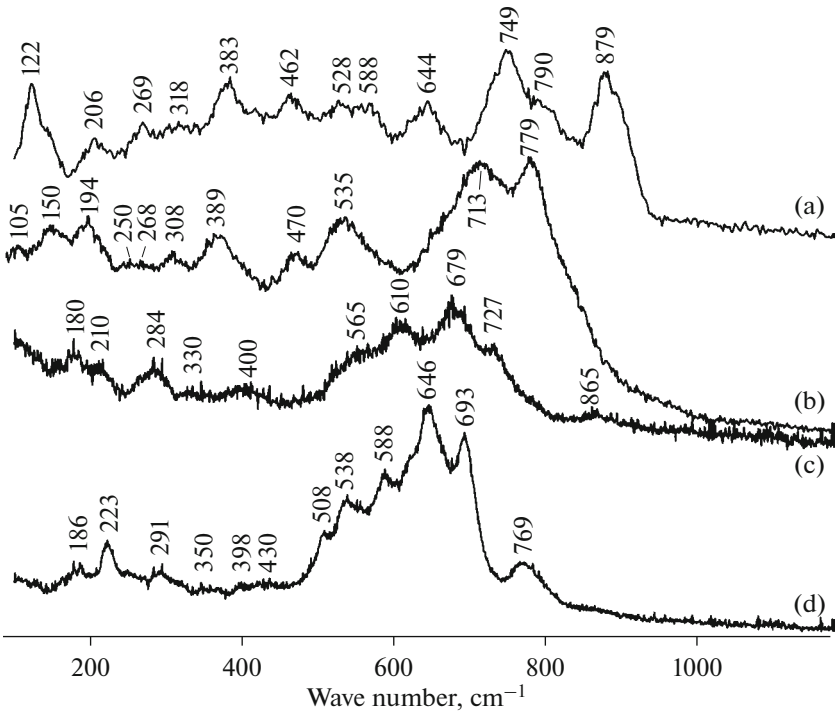

Fig. 7. Raman spectra of (a) hibonite $Ca_{1.0}(Al_{10.2}Fe_{0.9}Ti_{0.6}Mg_{0.3})O_{19}$ from Tashelga occurrence, Mountain Shoriya, Russia, (b) Al-analogue of yimengite from Obnazhennaya pipe, (c) nežilovite from Nežilovo, and (d) Mn-analogue of plumboferrite from Nežilovo.

between the Ti–O and Al–O stretching vibrations. In this case, the charge balance is provided by the simultaneous incorporation of Mg^{2+} and Ti^{4+} in the mineral structure.

IR spectroscopy. Two groups of strong bands are identified in the IR spectra of MGM (Figs. 9, 8). The higher frequency bands (in the ranges of 700–900 cm^{-1} for diaoyudaoite and hibonite, 600–800 cm^{-1} for Al-bearing nežilovite, and 500–700 cm^{-1} for Al-free MGM) are attributed to stretching vibrations in polyhedra with low coordination numbers (4 and 5), while lower frequency bands (in the range of 500–700 cm^{-1} for diaoyudaoite and hibonite and 400–500 cm^{-1} for the Al-depleted MGM) are assigned to stretching vibrations involving octahedrally coordinated cations. The individual bands within these ranges are well resolved in the IR spectrum of the stoichiometric pure diaoyudaoite, are slightly poorer in the spectra of hibonite and barioferrite, and significantly overlap in the spectra of nežilovite, lindqvistite, and plumboferrite. The positions of the absorption maximums of the strongest bands within the ranges of the stretching vibrations of the tetrahedral, bipyramidal, and octahedral groups are shifted towards lower frequency region with increasing average weight of the *M* cations: 599 and 768 cm^{-1} for diaoyudaoite (Al), 594 and 753 cm^{-1} for hibonite (predominantly Al with minor Fe and Ti), 462 and 617 cm^{-1} for nežilovite (predominantly Fe with subordinated Mn, Zn, and Al), 405–433 and 549–582 cm^{-1} for barioferrite, lindqvistite, and magnetoplumbite (predominantly Fe, partly with minor Mn and/or Ti). The comparison of the IR spectra of barioferrite, lindqvistite, and magnetoplumbite (Fig. 9) shows that the substitution of Fe^{3+} and Pb^{2+} cations by lighter cations (Mg^{2+} and Ba^{2+}, respectively) results in the band shift within both ranges to the higher frequency region.

The bands with frequencies below 500 cm^{-1} are attributed to lattice vibrations involving *A* cations with low force-strength characteristics. The weak bands with frequencies above 1000 cm^{-1} are referred to overtone and combination modes.

DISCUSSION

The above data are referred to MGM from geochemically different environments. Uncommon formation conditions led to the origin of MGM whose compositions correspond to the new mineral species belonging to the magnetoplumbite group, Ba analogue of nežilovite, Mn analogue of plumboferrite, and Al analogue of yimengite.

The compositional variations of MGM are reflected in the vibrational spectra of the minerals while the position of spectral bands is determined by the average weight of the *M* cations.

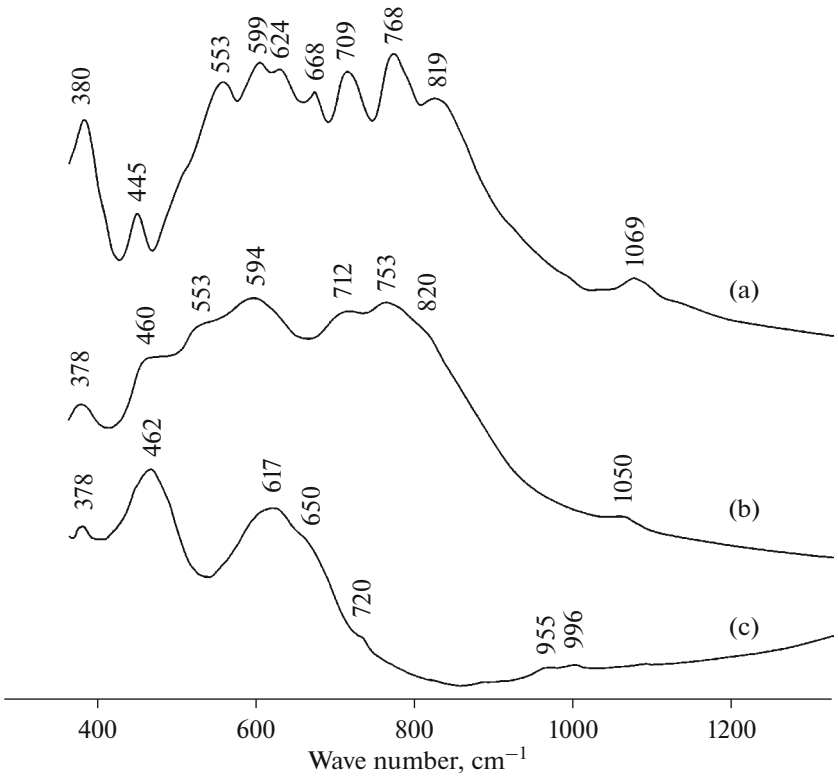

Fig. 8. IR spectra of Al-bearing MGM. (a) Technogenic diaoyudaoite from scoria of the Klyuchevskiy ferroalloy factory, Sverdlovsk oblast in Russia; (b) hibonite $Ca_{1.0}(Al_{10.2}Fe_{0.9}Ti_{0.6}Mg_{0.3})O_{19}$ from the Tashelga occurrence, Mountain Shoria; (c) nežilovite, $Pb_{1.0}(Fe_{5.7}Mn_{2.3}Zn_{2.0}Al_{1.3}Ti_{0.5}Sb_{0.2})O_{19}$ from Nežilovo.

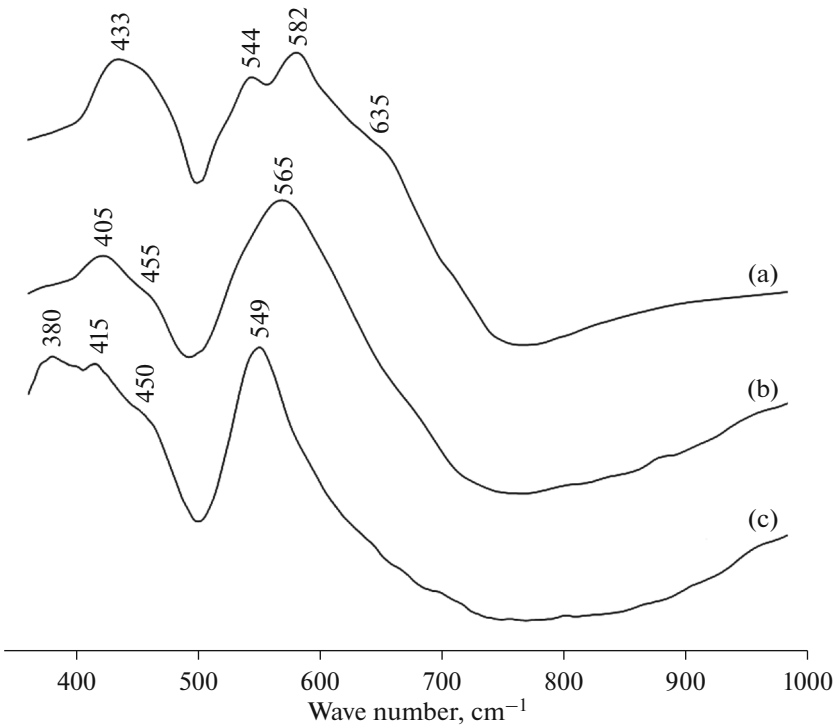

Fig. 9. IR spectra of Al-free and Al-poor MGM: (a) barioferrite $Ba_{0.95}Fe_{12.03}O_{19}$ from the Hatrurim Formation, Israel, (b) lindqvistite $Pb_{2.0}(Fe_{14.8}Mn_{1.4}Mg_{0.8})O_{27}$ from the Jakobsberg deposit, Sweden, and (c) magnetoplumbite $(Pb_{0.95}Ba_{0.05})(Fe_{8.1}Mn_{3.0}Ti_{0.8}Al_{0.1})O_{19}$ from the Långban deposit, Sweden.

The strongest lower frequency shifts of spectral bands attributed to the vibrations of the metal–oxygen tetrahedra and octahedra are observed for the Pb-dominated MGM with low content of the light *M* cations, Al and Mg (see also: Konzett et al., 2005; Yang et al., 2007).

As can be seen from the IR spectroscopic data, the bands in the IR spectra are broad and poorly resolved in the MGM samples with the compositions quite different from those of the endmembers. Obviously, it is caused by cation disordering and mixed-occupied sites in such minerals.

Furthermore, a serious error in the article focused on the vibrational spectroscopy of nežilovite (Stamatovska et al., 2011) should be mentioned. The authors of that paper enthusiastically noted that the strongest band in the measured Raman spectrum of nežilovite whose intensity is much higher than that of the other bands is observed at the very high frequency of 1099 cm^{-1}. In the cited paper, this band was attributed to "the complex mode involving consistent movement with the metal–oxygen octahedra." Taking into account unconventional terminology, the sense of this attribution is not clear. It is possible that combination mode is feasible, but in this case, it should be expected that the corresponding band has very low intensity. Actually, this "anomaly" has a simple explanation: the authors of the cited paper measured Raman spectra of dolomite associated with nežilovite rather than that of nežilovite itself. Thus, the Raman spectrum of nežlovite was measured for the first time in this study.

ACKNOWLEDGMENTS

We thank E.E. Laz'ko for the collection of deep xenoliths contributed to the Mineralogy Division, Moscow State University; O.G. Safonov, V.K. Garanin, and I.V. Pekov for useful discussion; N.A. Nekrylov, L.Yu. Kadebskaya, and Center of Common Use at the Petrology Division, Moscow State University for their assistance in the measurement of Raman spectra; and N.N. Korotaeva for the preliminary electron microprobe study of the xenolith from the Obnazhennaya pipe.

FUNDING

This study was supported by the Russian Foundation for Basic Research, grant no. 18-05-00051_a.

REFERENCES

Anan'ev, S.A., Konovalenko, S.I., Rastsvetaeva, R.K., Aksenov, S.M., Chukanov, N.V., Sapozhnikov, A.N., Zagorsky, V.E., and Virus, A.A., Tashelgite, CaMg$Fe^{2+}Al_9O_{16}(OH)$, a new mineral species from calcareous scarns in Gorny Shoria, *Geol. Ore Deposits*, 2011, vol. 53, no. 1, pp. 751–757.

Back, M.E., *Fleischer's Glossary of Mineral Species, Tucson: The Mineralogical Record Inc.,* 2014.

Barić, L., Piemontit, gahnit und rutil aus dem Fundort der Blei und Zinkerze bei dem Dorfe Nezilovo in Mazedonien, *Glasnik Prirodnjackog Muzeja, Beograd, Ser. A*, 1960, vol. 13, pp. 200–204.

Bermanec, V., Holtstam, D., Sturman, D., Criddle, A.J., Back, M.E., and Ščavničar, S., Nežilovite, a new member of the magnetoplumbite group, and the crystal chemistry of magnetoplumbite and hibonite, *Can. Mineral.*, 1996, vol. 34, pp. 1287–1297.

Chukanov, N.V., Aksenov, S.M., Jančev, S., Pekov, I.V., Göttlicher, J., Polekhovsky, Yu.S., Rusakov, V.S., Nelyubina, Yu.V., and Van, K.V., A new mineral species ferricoronadite, $Pb[Mn_6^{4+}(Fe^{3+}Mn^{3+})_2]O_{16}$: mineralogical characterization, crystal chemistry and physical properties, *Phys. Chem. Mineral.*, 2016, vol. 43, no. 7, pp. 503–514.

Chukanov, N.V., Krzhizhanovskaya, M.G., Jančev, S., Pekov, I.V., Varlamov, D.A., Göttlicher, J., Rusakov, V.S., Polekhovsky, Y.S., and Ermolaeva, V.N., Zincovelesite-6*N*6*S*, IMA 2017-034. CNMNC Newsletter. 2017. no. 38. P. 1037. *Miner. Mag.*, 2017, vol. 81, pp. 1033—1038.

Chukanov, N.V., Jančev, S., and Pekov, I.V., The association of oxygen-bearing minerals of chalcophile elements in the orogenetic zone related to the "Mixed Series" complex near Nežilovo, Republic of Macedonia, *Macedonian J. Chem. Chemical Eng.*, 2015, vol. 34, no. 1, pp. 115–124.

Chukanov, N.V., Zubkova, N.V., Schäfer, C., Varlamov, D.A., Ermolaeva, V.N., Polekhovsky, Yu.S., Jančev, S., Pekov, I.V., and Pushcharovsky, D.Yu., Ferriakasakaite-(La): new data, new findings and crystal-chemical relationships with other epidote-supergroup minerals, *Europ. J. Mineral*, 2018.

Ermolaeva, V.N., Chukanov, N.V., Jančev, S., and Van, K., Endogenic oxide parageneses with chalcophile elements in the orogenetic zone related to the "Mixed Series" of the Pelagonian massif, Republic of Macedonia, *New Data on Minerals*, 2016, vol. 51, pp. 12–19.

Ermolaeva, V.N., Varlamov, D.A., Jančev, S., and Chukanov, N.V., Spinel-group and högbomite-supergroup minerals from a nonsulfide endogenous Pb–Zn–Sb–As association in the Pelagonian massif, Macedonia, *Zap. Ross. Mineral. O-va*, 2018, no. 3, pp. 27–43.

Grey, I.E., Velde, D., and Criddle, A., Haggertyite, a new magnetoplumbite-type titanate mineral from the Prairie Creek (Arkansas) lamproite, *Am. Mineral.*, 1998, vol. 83, pp. 1323–1329.

Haggerty, S.E., Grey, I.E., Madsen, I.C., Criddle, A.J., Stanley, C.J., and Erlank, A.J., Hawthorneite, $Ba[Ti_3Cr_4Fe_4Mg]O_{19}$: a new metasomatic magnetoplumbite-type mineral from the upper mantle, *Am. Mineral.*, 1989, vol. 74, pp. 668–675.

Holtstam, D., Norrestam, R.A., and Sjödin, A., *Plumboferrite: new mineralogical data and atomic arrangement, Am. Mineral.*, 1995, vol. 80, pp. 1065–1072.

Jančev, S., Chukanov, N.V., and Ermolaeva, V.N., Association of oxide minerals – concentrators of chalcophile elements (Pb, Zn, Sb) from the "Mixed series" near Nezilovo village, Macedonia, *Mat. Third Congress of Geologists of Republic of Macedonia, Struga,* 2016, vol. 2, pp. 401–404.

Konzett, J., Yang, H., and Frost, D.J., Phase relations and stability of magnetoplumbite-and crichtonite-series phases under upper-mantle PT conditions: an experimental study to 15 GPa with implications for LILE metasomatism in the lithospheric mantle, *J. Petrol.*, 2005, vol. 46, pp. 749–781.

Lengauer, C.L., Tillmanns, E., and Hentschel, G., Batiferrite, $Ba[Ti_2Fe_{10}]O_{19}$, a new ferromagnetic magnetoplumbite-type mineral from the Quaternary volcanic rocks of the western Eifel area, Germany, *Mineral. Petrol.*, 2001, vol. 2001, pp. 1–19.

Ma C. Hibonite-(Fe), $(Fe,Mg)Al_{12}O_{19}$, a new alteration mineral from the Allende meteorite. *Amer. Miner.* 2010. Vol. 95. P. 188–191.

Murashko, M.N., Chukanov, N.V., Mukhanova, A.A., Vapnik, E., Britvin, S.N., Krivovichev, S.V., Polekhovsky, Yu.S., and Ivakin, Yu.D., Barioferrite $BaFe^{3+}_{12}O_{19}$: a new mineral species of the magnetoplumbite group from the Hatrurim Formation in Israel, *Geol. Ore Deposits*, 2011, vol. 53, no. 7, pp. 558–563.

Obradors, X., Collomb, A., Pernet, M., Samaras, D., and Joubert, J.C., X-ray analysis of the structural and dynamic properties of $BaFe_{12}O_{19}$ hexagonal ferrite at room temperature, *J. Solid State Chem.*, 1985, vol. 56, pp. 171–181.

Stäblen, H., *Hard ferrites and plastiferrites, Ferromagnetic Materials*, Ed. by E. P. Wohlfarth, 1982, vol. 3, pp. 441–602.

Stamatovska, N., Makreski, P., Pejov, L., and Jovanovski, G., Minerals from Macedonia. XXVII: theoretical and experimental study of the vibrational spectra of endemic nezilovite, *J. Molec. Struct*, 2011, vol. 993, no. 1, pp. 104–108.

Townes, W.D., Fang, J.H., and Perrotta, A.J., The crystal structure and refinement of ferromagnetic barium ferrite, *Z. Kristallogr*, 1967, vol. 125, pp. 437–449.

Varlamov, D.A., Ermolaeva, V.N., Jancev, S., and Chukanov, N.V., Pyrochlore-supergroup minerals from a nonsulfide endogeneous association of Pb–Zn–Sb–As minerals in the Pelagonian massif, Macedonia, *Zap. Ross. Mineral. O-va*, 2017, no. 4, pp. 65–78.

Peng Zhizhong and Lu Qi, The crystal structure of yimengite, *Sci. Geol. Sinica*, 1985, vol. 28, pp. 882–887.

Translated by I. Baksheev